Large band-gap bowing in Cu$_{1-x}$Ag$_x$GaS$_2$ chalcopyrite semiconductors and its effect on optical parameters

Chandrima Mitra and Walter R. L. Lambrecht

Department of Physics, Case Western Reserve University, Cleveland, Ohio 44106-7079, USA

(Received 13 April 2007; published 18 July 2007)

The band-gap bowing in the Cu$_{1-x}$Ag$_x$GaS$_2$ chalcopyrite alloy is studied using the full-potential linearized muffin-tin orbital method combined with various structural models, including so-called special quasirandom structures. The calculations confirm a large band-gap bowing ($\sim$0.7 eV) in agreement with recent experimental results. It is found that the large bowing in part arises from a nonlinear behavior of the c/a ratio with concentration. Layered structures are found to have similar bowing to special quasirandom structures. The nonlinear band-gap behavior also leads to a nonlinear behavior of the index of refraction and the second-order nonlinear optical susceptibility with concentration. The maximum $\chi^{(2)}$ is found for a 50% alloy and is calculated to be about 27 pm/V.

PACS number(s): 71.20.Nr, 78.20.Ci

I. INTRODUCTION

Chalcopyrite semiconductors offer another versatility compared to the standard III-V and II-VI semiconductors. In particular, Cu(Ga,In)(S,Se)$_2$ have found applications in thin-film photovoltaic solar energy conversion.[1] AgGa(S,Se,Te)$_2$ compounds, on the other hand, have found applications in nonlinear optics as frequency converters.[2] Crucial alternative features of these chalcopyrite structure compounds are (1) their reduced symmetry (tetragonal instead of cubic) which allows for birefringence and is important for phase matching in the nonlinear optical applications; (2) the presence of d bands of the group-I element which modifies the nature of the states near the band gap. The latter plays, for example, a role in the defect physics in these materials which is one of the reasons for their success in photovoltaic applications.[3] As usual, to fine-tune the properties of these semiconductors, it is of interest to make alloys among them by substituting various cations or anions. In this paper, we study the effect of substituting the group-I element, Ag versus Cu. The Cu$_{1-x}$Ag$_x$GaS$_2$ alloy system is chosen as an example because of the recent reports of a large band-gap bowing in this system.[4,5] The band-gap bowing defines the deviation from linearity of the band gap as function of concentration. Furthermore, the two experimental reports gave somewhat different results on the band-gap bowing, or more particularly on the concentration at which the minimum band gap occurs. Whereas Choi *et al.*[4] places this minimum gap concentration at about 50%, Matsushita *et al.*[5] place it at about 30%. Earlier work[6] reported a smaller bowing for this alloy system. Also, for the corresponding selenide system, smaller bowing parameters were reported by Park *et al.*[7] The question arises how this band-gap bowing is related to the underlying structural properties. A large bowing offers the possibility to strongly modify the properties of the alloy system. The indices of refraction are some of the most important optical properties for designing frequency conversion systems. The nonlinear optical coefficient is also important. Often it is assumed that these parameters vary simply linearly with concentration. An important purpose of this paper is to test the validity of this assumption.

The paper is organized as follows. In Sec. II, we describe our computational approach. In Sec. III, we define the structures investigated, in particular, how to deal with the problem of simulating a random alloy. In Sec. IV, we first give our results for the structural properties and band structures of the end compounds CuGaS$_2$ and AgGaS$_2$ (Sec. IV A). Next, we discuss the behavior of the lattice constants and band-gap bowing in the alloy system (Sec. IV B). We will show, in particular, that the bowing of the c/a ratio is in part responsible for the large band-gap bowing. Finally, we discuss the effects on the optical properties as function of concentration in Sec. IV C. We summarize the results in Sec. V.

II. COMPUTATIONAL APPROACH

The underlying theoretical approach is density functional theory in the local density approximation.[8] To solve the Kohn-Sham equations, we use the the full-potential linearized muffin-tin orbital (FP-LMTO) method as implemented by van Schilfgaarde and Methfessel.[9] This approach is an all-electron approach without shape approximation. It makes use of an efficient minimal basis set of augmented smooth Hankel functions.[10] The parameters in the basis set include the Hankel function decay lengths or (kinetic energies) κ^2 and the smoothing radii R_{sm}, which make the basis functions curve over just outside the muffin-tin radius and help to give the basis functions their optimum shape. These parameters along with the angular momentum cutoffs are optimized at the start of the calculations by minimizing the non-self-consistent Harris-Foulkes functional.[11,12] In the present calculations, we employ a basis set consisting of a single spd channel per atom. However, for Ga, the semicore $3d$ orbitals are added as "local orbitals."[13] For Cu and Ag, of course, the $3d$ and $4d$ orbitals are treated as valence states. The various quantities such as charge density, wave functions, and potential are separated in a smooth part, tabulated on a regular mesh in real space, and their augmentation counterparts inside the spheres subtract a local expansion of the smooth function and replace it by the actual quantities inside the spheres. The fast Fourier transform technique is used to solve Poisson's equation for the smooth part. The regular mesh

used is a $40 \times 40 \times 40$ mesh for the primitive body centered tetragonal cell. The mesh is correspondingly increased for the supercells used. To sample the Brillouin zone for the self-consistent calculations and atomic relaxation, a shifted and symmetrized Monkhorst-Pack[14] $2 \times 2 \times 2$ mesh is used and was found to be sufficiently converged.

For the optical calculations, we used the atomic sphere approximation (ASA) to the LMTO method because the calculation of optical matrix elements has not yet been implemented in the FP-LMTO code. In this method, slightly overlapping spheres are used instead of touching muffin-tin spheres and the potential is spherically averaged inside the sphere as well as the charge density. The latter approximation is insufficient to obtain structural energy differences but is still quite accurate for the band structure. Empty spheres are introduced to make the system close packed and avoid too large overlaps of the space filling spheres. In any case, since we have the FP-LMTO band structures available for comparison, we can check explicitly that the ASA works fine for the bands of these materials. We calculate the imaginary part of the dielectric function in the long-wavelength limit random-phase approximation,

$$\epsilon_2^j(\omega) = \left(\frac{2\pi e}{m\omega} \right)^2 \sum_k |\langle vk|p^j|ck \rangle|^2 \delta(E_c(k) - E_v(k) - \hbar\omega),$$

$$(1)$$

with $p^j = -i\hbar\nabla_j$ the momentum operator, using Gaussian units. Local-field effects and excitonic effects are neglected. The real part of the dielectric function is then obtained by Kramers-Kronig transformation and the index of refraction is calculated from the square root of the complex dielectric function and taking the real part.

To calculate the nonlinear $\chi^{(2)}$, we use the approach of Sipe and co-workers[15,16] as implemented in Rashkeev et al.[17] The $\chi^{(2)}$ is separated in a pure interband contribution and a mixed intraband interband contribution, which we will call intraband for short. These usually have opposite signs and similar magnitudes. In previous work on the I-III-VI$_2$ compounds,[18,19] we discussed in detail how these two contributions play a role in establishing which materials have the higher $\chi^{(2)}$. Because of Kleinman symmetry in the static limit, only one component of the third-order tensor needs to be calculated, namely the $\chi_{x,yz}^{(2)} = 2d_{14}$.

Both linear and even more so nonlinear optics depend crucially on the band gap. Since local density approximation (LDA) usually underestimates the band gaps, we need to add a band-gap correction. This is done in the linear optics case simply by shifting the imaginary part of ϵ up by a constant before evaluating the real part. This procedure is equivalent to inserting a so-called scissor operator, i.e., a shift with projection on the conduction bands. This should be accompanied by a renormalization of the matrix elements as argued by Levine et al.[20] The scissor shift is implemented in this manner for the nonlinear optical calculations. It should be kept in mind that nonlinear optics is more sensitive to computational details, such as the k-point sampling. The k-point sampling for the linear and nonlinear optical calculations is carried out using the tetrahedron method[21] and with a large

number of k points than used for the self-consistency calculations, for instance, a $10 \times 10 \times 10$ mesh for the standard unit cell of chalcopyrite.

III. STRUCTURAL MODELS

The key question in modeling alloys is how to deal with the randomness of the atomic substitutions. An efficient way to deal with this question is to use the so-called special quasirandom structures (SQSs).[22] These are relatively small ordered supercells designed such that their correlation functions mimic the ensemble average of a random alloy, i.e., $\bar{\Pi}_{k,m} = (2x-1)^k$. Here, $\bar{\Pi}_{k,m}$ is a correlation function, i.e., a lattice sum over spin products (or figures) corresponding to a certain order k and a certain neighbor distance m. The underlying idea is that the ensemble average of any quantity of interest can be expanded in these correlation functions,

$$\langle P \rangle = \sum_{k,m} \langle \bar{\Pi}_{k,m} \rangle P_{k,m}, \tag{2}$$

where $P_{k,m}$ are the so-called interaction parameters. The number of terms needed in this expansion obviously depends on the property studied and the size of the interaction parameters for the system at hand. The quality of a SQS is determined by the distance and order up to which the deviations from the random correlation functions vanish and how small the remaining deviations are. Equivalently, one defines the Warren-Cowley[23] short-range order parameter

$$\alpha_j = 1 - \frac{P_B(j)}{x_B}, \tag{3}$$

in which $P_B(j)$ is the probability to find a B atom as jth nearest neighbor site of an A atom at the origin. The relation between this short-range order parameter and the spin correlation function is[24]

$$\alpha_j = \frac{\langle \bar{\Pi}_{2,j} \rangle - q^2}{1 - q^2}, \tag{4}$$

with $q = 2x - 1$.

We used a 64 atom supercell, which is a $2 \times 2 \times 1$ superlattice of the face centered tetragonal cell of chalcopyrite. It thus contains 16 group-I sites which are populated with either Ag or Cu atoms. The group-I atoms in the chalcopyrite fct cell occur at reduced coordinate positions $(0,0,0)$, $(0,0.5,0.25)$, $(0.5,0.5,0.5)$, and $(0.5,0,0.75)$. The remaining Ga and S atoms are merely spectator atoms in terms of the alloy disorder. A computer code[25–28] is used for generating the SQS. It uses iterative switching of atomic pairs in a Metropolis-type algorithm until the deviations from the random correlation functions are minimized. The structures obtained are specified by giving the positions of the Ag and Cu atoms, respectively, as given in Table I. We constructed 25% and 50% alloys, and then simply reversed the Cu and Ag atoms to obtain a 75% alloy model.

The quality of the SQS is given by the deviations of the correlation functions from the random one, or for the pair correlation functions by the Warren-Cowley parameters.

TABLE I. Reduced coordinates of the A and B atoms in a 25% and 50% $2\times2\times1$ SQS of the chalcopyrite group-I sublattice.

	$x=1/4$				$x=1/2$		
A1	0	1	0	A1	0	3/2	1/4
A2	0	3/2	1/4	A2	1/2	0	3/4
A3	3/2	0	3/4	A3	1/2	1/2	1/2
A4	3/2	1	3/4	A4	1/2	1	3/4
B1	0	0	0	A5	1/2	3/2	1/2
B2	0	1/2	1/4	A6	1	1	0
B3	1/2	0	3/4	A7	3/2	1/2	1/2
B4	1/2	1/2	1/2	A8	3/2	1	3/4
B5	1/2	1	3/4	B1	0	0	0
B6	1/2	3/2	1/2	B2	0	1/2	1/4
B7	1	0	0	B3	0	1	0
B8	1	1/2	1/4	B4	1	0	0
B9	1	1	0	B5	1	1/2	1/4
B10	1	3/2	1/4	B6	1	3/2	1/4
B11	3/2	1/2	1/2	B7	3/2	0	3/4
B12	3/2	3/2	1/2	B8	3/2	3/2	1/2

These are given in Table II. Since no first neighbor triplets occur in this sublattice, unlike in fcc, we do not consider triplet and higher correlation functions. The strongest deviation from random behavior occurs for the fourth neighbor shell in the 25% SQS. The quality of the SQS could be further improved by taking a 128 atom $2\times2\times2$ cell. In that case, we can make all $\alpha_j=0$ up to sixth neighbors for the 25% case. However, as we will see below, the disorder of the structure appears to affect the band-gap bowing only slightly, so we have not pursued these large cells yet.

To further check the influence of the structural disorder, we also studied simple layered structures in the c direction. Here, we used simple 16 atom (face centered tetragonal or fct) cells containing four group-I cations. For the 25% and 75% cases, there is obviously only one way to this. For the 50% composition, we can either have AgCuAgCu or a AgAgCuCu arrangement. We investigate both.

IV. RESULTS

A. CuGaS$_2$ and AgGaS$_2$

First, we present our results for the end compounds of the alloy series to establish the accuracy of our calculations. Structural relaxation of the internal parameter u, which

TABLE II. Short-range order Warren-Cowley parameters α_j for the SQS defined in Table I.

x	Neighbor shell j					
	1	2	3	4	5	6
1/4	0	0	−1/12	−1/3	0	−1/12
1/2	0	0	−1/8	0	0	−1/8

TABLE III. Lattice parameters, bulk modulus, and band gap of CuGaS$_2$ and AgGaS$_2$.

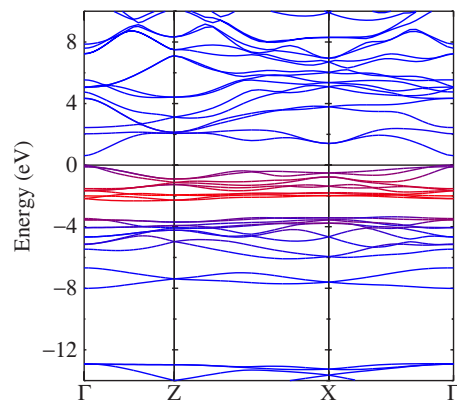|	CuGaS$_2$		AgGaS$_2$	
	Theor.	Expt.	Theor.	Expt.
a (Å)	5.345	5.35	5.747	5.75
$\eta=c/(2a)$	0.9795	0.98	0.892	0.895
u	0.2489	0.2539	0.284	0.2908
$d_{\text{I-S}}$	3.23	3.24	3.37	3.387
$d_{\text{Ga-S}}$	3.234	3.226	3.19	3.18
B (GPa)	85.2	95.8[a]	68.6	77.6[a]
E_g (eV)	0.8	2.47	1.01	2.72

[a]Reference 29.

specifies essentially the relative bond lengths of the Cu–S or Ag–S and Ga–S bond lengths as well as the $\eta=c/(2a)$ and a lattice constants were carried out. The bond lengths in the ABC_2 compound are related to the u parameter as follows:

$$d_{AC} = a\sqrt{\left(\frac{1}{4}\right)^2 + u^2 + \frac{\eta^2}{4}},$$

$$d_{BC} = a\sqrt{\left(\frac{1}{4}\right)^2 + \left(\frac{1}{2}-u\right)^2 + \frac{\eta^2}{4}}. \quad (5)$$

Table III gives the calculated lattice structural parameters and the bulk moduli compared with experiment. Excellent agreement is obtained. We note, in particular, that the c/a ratio in the Ag compound is significantly lower than in the Cu compound. As we will see below, the c/a ratio is an important parameter in these materials. The band gaps are underestimated because of the LDA and are found to be direct at the Γ point in both cases.

In Figs. 1 and 2, the band structures are plotted for CuGaS$_2$ and AgGaS$_2$, respectively. The k points shown are $Z=\left(0,0,\frac{4\pi}{c}\right)$, $\Gamma=(0,0,0)$, and $X=\frac{\pi}{a}(1,1,0)$ In this figure, we have highlighted the group-I d bands by coloring the bands as a mixture of red and blue with the red contribution proportional to the d-orbital contribution to the Bloch state at

FIG. 1. (Color online) The band structure of CuGaS$_2$ highlighting the Cu d bands in red.
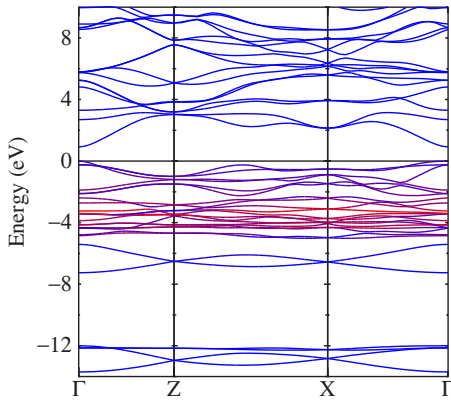
FIG. 2. (Color online) The band structure of AgGaS$_2$ highlighting the Ag d bands in red.

that each k point. Thus pure d bands are red, bands with zero d contribution are blue and band with a mixed d and other orbital character are purple. The purple bands near the valence band maximum are a mixture of Cu-d and S-p, whereas some almost purely d bands occur at lower energy. In CuGaS$_2$, a gap occurs just below these bands, whereas in AgGaS$_2$, no such gap is present. We can clearly see that the Ag-d bands are significantly lower in energy than in Cu. This means that they push up the valence band S-p states less in Ag than in Cu and this results in a higher band gap for the Ag than the Cu compound. This is a somewhat unusual circumstance because usually materials with heavier atoms and hence larger lattice constants tend to have lower band gaps. Ultimately, this is related to the stronger relativistic effects on the Ag-d bands.

Using a similar color coding approach, we can analyze the nature of the conduction band minimum. We find that it is primarily composed of Ga-s, S-s, and S-p, but not Cu-s. The latter appears to be more dominant a few eV higher in the conduction bands. Hence, the conduction band minimum is little influenced by the choice of group-I cation.

B. Alloy properties

With the above established background on the end compounds, we now proceed to the alloy system. First, we examine the results of the 16 atom layered structures. In Fig. 3, we show the lattice constants a and c and their ratio $\eta = c/2a$ as function of concentration, compared to the experimental data of Matsushita et al.[5] For the 50% case, the results of the two different structural models, switching every layer or every two layers, agree to within the precision of the calculations, so they are not shown separately. We notice that while a follows linear Vegard's law[30], the c lattice constant behaves nonlinear and has an upward bowing. In fact, c initially increases. This is, in part, due to the fact that η decreases and a increases with x. Thus, even if both would behave linear, there would already be a quadratic term. This is insufficient, however, to explain the behavior, as is shown by the dashed-dotted line in the upper panel. A significant fraction of the upward bowing of c is due to an upward bowing of η.
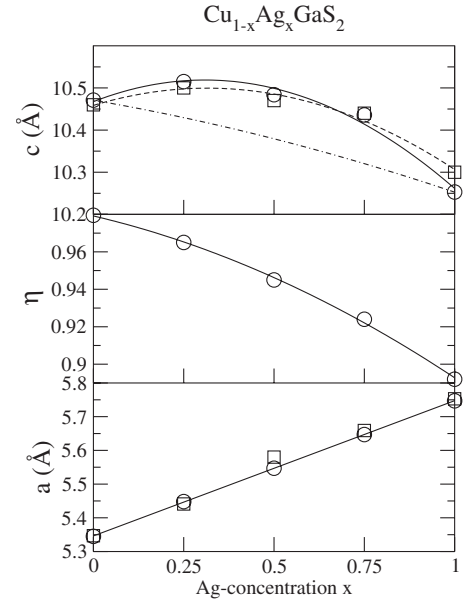

FIG. 3. Variation of the lattice constants a and c and their ratio $\eta = c/(2a)$ with Ag concentration x. Circles represent calculated points, squares represent experimental points from Ref. 5. The continuous lines are linear (for a) or quadratic fits (for η and c) to the calculated data, and the dashed-dotted line in the top figure is what would be obtained with linear η and a.

The reason for the η behavior is presently not clear. While the trends of lattice constants a and internal parameter u in chalcopyrites can be nicely rationalized in terms of the idea of conservation of tetrahedral bonds,[31] the trends in c/a ratio are less clear. One idea that was proposed in the past is that it is related to conservation of tetrahedral bond angles.[33] However, one cannot preserve all bond angles to stay tetrahedral and thus, the relation between u and η depends somewhat arbitrary on which bond angles are chosen to be conserved. Also, Jaffe and Zunger[31] showed that including a relation like this gives only mediocre predictions for the trends in η. This indicates that long-range forces rather than local bond considerations influence c/a.

In Fig. 4, we show that this has an important effect on the band-gap bowing. The band band-gap bowing is significantly larger if we include the nonlinear c/a than when we assume a linear c/a behavior. The bowing coefficient is as usual defined as b in the expression

$$E_g(x) = xE_A + (1-x)E_B - bx(1-x). \qquad (6)$$

Quadratic fits to the data points are included in the figure and lead to a band-gap bowing coefficient of about 0.5 for the linear c/a case and 0.7 for the relaxed nonlinear c/a case. Again, in these figures, the two possible 50% layered structure gave identical results to within the precision of the calculation.

Next, we examine the effects of randomness. In this case, we maintain the c/a ratios as established from the layered compounds but now use the 64 atom SQS structures in which the group-I cations are intermixed in each layer. The resulting band gap as function of concentration is shown in
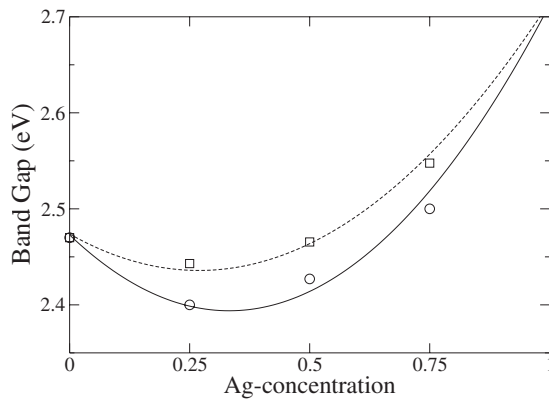
FIG. 4. Variation of the band gap with Ag concentration x, using the layered structures. Squares, calculated points with linear c/a; circles, calculated points with optimized nonlinear c/a. The solid and dashed lines are quadratic fits.

Fig. 5 and compared with the previous results. Both calculations use the same c/a ratios. Although the individual points differ slightly, the fitted quadratic curves are rather close to each other and thus the band-gap bowing coefficient is found to be almost the same as obtained from the layered systems. This is somewhat surprising and indicates that there is little room for band-gap engineering by structuring the materials in segregate layers as opposed to a random alloy.

In both Figs. 4 and 5 we added a gap correction to the LDA gaps which is taken to vary linear between the end compounds. Thus, it does not contribute to the bowing parameter. Finally, we note that we find a minimum band gap at $x=0.33$, closer to the results of Matsushita et al.[5] than to Choi et al.[4] We note that within the quadratic approximation, $x_{min}=0.5$ will only occur for infinite bowing parameter or equal gaps on both ends, but of course the bowing could be stronger than quadratic.

The origins of band-gap bowing have been studied previously by, e.g., Zunger and Jaffe.[32] They found it useful to decompose the band-gap bowing in a volume deformation contribution, i.e., arising from the compression and expansion of the two end compounds to the average lattice constant of the alloy, a chemical substitution contribution at
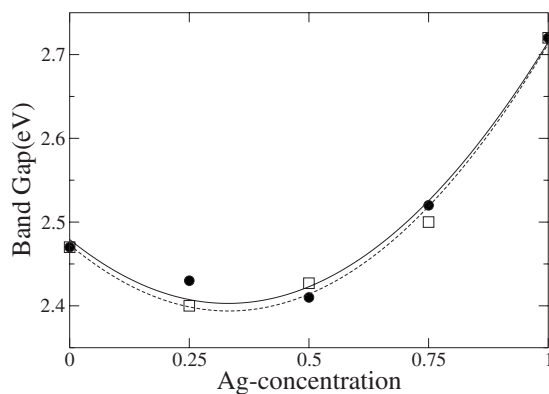

FIG. 5. Variation of the band gap with Ag concentration x, using the special quasirandom structures, filled circles and solid line; using the layered structure, open squares, and dashed line.
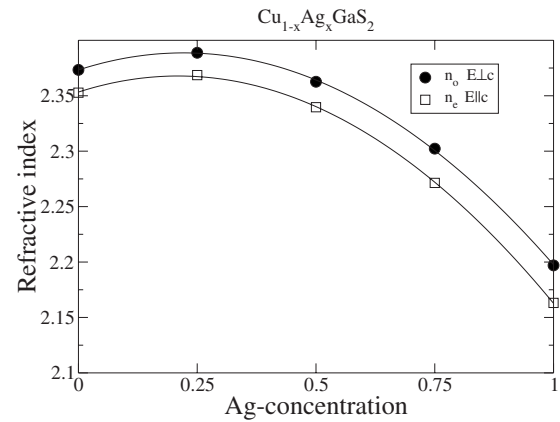

FIG. 6. Variation of the refractive indices with Ag concentration x. Filled circles: ordinary index ($E \perp c$) and extraordinary index ($E \| c$).

fixed equilibrium lattice constant of the alloy, and a relaxation contribution. The volume deformation contribution can be written as

$$b_{VD} = \frac{E_g(A, a_{eq}^A) - E_g(A, a_{av})}{x} + \frac{E_g(B, a_{eq}^B) - E_g(B, a_{av})}{(1-x)},$$
(7)

with $a_{eq}^{A,B}$ the equilibrium lattice constant of each compound $A = \text{AgGaS}_2$ $B = \text{CuGaS}_2$, and a_{av} the average one for the alloy composition x. In the present case, this amounts to $b_{VD} \approx 0.2$ eV.

The pure chemical mixing contribution could be defined as

$$b_{CM} = \frac{E_g(A, a_{av})}{x} + \frac{E_g(B, a_{av})}{(1-x)} - \frac{E_g(A_{1-x}B_x, a_{av}, \eta_{av}, u_{av})}{x(1-x)},$$
(8)

in which the structural parameters are all linearly averaged between the end compounds. Instead, we have calculated $b_{CM} + b_{rel}$ including the relaxation contribution by replacing η and u by their relaxed values in the final term. This term then amounts to about 0.5 eV. This accounts for the total bowing of about 0.7 eV. The relaxation contribution could be split further in a contribution due to the relaxation of the internal coordinate u and due to the c/a relaxation. We have already seen here that the u relaxation gives rise to a change in bowing parameter of about 0.2 eV.

C. Optical properties

In this section, we address the question of the variation of the optical properties with concentration. First, we examine the indices of refraction (at zero frequency), i.e., well below the band gap, but not including the lattice vibrational contributions, as function of Ag concentration (Fig. 6).

They are clearly seen to have an upward bowing. This is not surprising since the dielectric function contains terms inversely proportional to the interband transitions or the gap. Nevertheless, the index of refraction is a somewhat more

TABLE IV. The second-order nonlinear coefficient $\chi^{(2)}_{x,yz}$ (in pm/V) as function of Ag concentration in $Cu_{1-x}Ag_xS_2$ alloys and their corresponding intraband and interband contributions.

x	$\chi^{(2)}$ (Calc.)	$\chi^{(2)}$ (Expt.)	Interband	Intraband
0.00	15.04	14[a]	−19.56	34.61
0.25	19.45		−24.85	44.30
0.50	27.31		−16.74	44.05
0.75	24.41		−6.05	30.46
1.00	18.78	18[a]	−5.86	24.67

[a]Reference 34.

derived and averaged quantity, not affected only by the minimal gap but by various interband transitions and one might have expected some averaging out of this nonlinear effect. Clearly, however, this is not the case in this strongly bowing system. We also notice that the alloys stay negative birefringent over the whole concentration range, in agreement with experiment. The birefringence in this case does not vary much with concentration.

As far as the nonlinear optics is concerned, we first point out that there is some anomaly here to begin with. Usually, lower gap materials give higher $\chi^{(2)}$; however, in this case, the Cu compound has a lower $\chi^{(2)}$ in spite of having the lower gap. As was pointed out in earlier papers,[18,19] this is to some extent related to a larger compensation between the intra- and interband contributions in the Cu compound. The origin of this is too complex to trace back all the way to the band structures but since one of the major differences between the two materials is the position of the d bands, one may expect this to play a role. It is, thus, rather difficult to anticipate what will happen in the alloy system where both d bands will be present.

The results for $\chi^{(2)}$ are shown in Table IV and in Fig. 7. As previously pointed out,[19] the reason for the lower $\chi^{(2)}$ in $CuGaS_2$ compared to $AgGaS_2$ is that there is a larger compensation between the inter- and intraband contributions. Consistent with the larger gap in $AgGaS_2$, both the interband and intraband contributions in $AgGaS_2$ are somewhat smaller but their cancellation is less severe. The positive intraband contribution and total $\chi^{(2)}$ show an upward bowing, while the negative interband contributions shows a downward bowing. Apparently, the maximum $\chi^{(2)}$ occurs for about 50%. It is interesting to note that by alloying the system, one can achieve a value of $\chi^{(2)}$ as high as 27, compared to 15 and 19 for the end compounds. This amounts to an improvement by
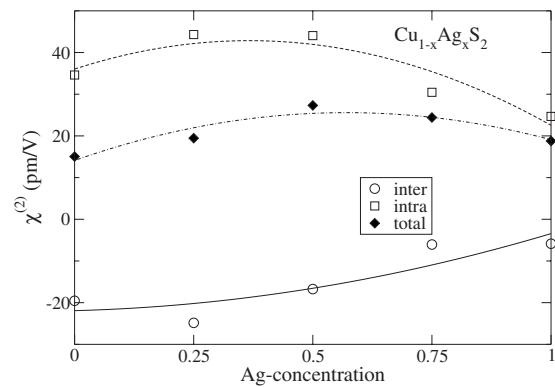

FIG. 7. Second-order nonlinear optical coefficient $\chi^{(2)}_{x,yz}$ in pm/V (filled diamonds) and its interband (open circles) and intraband (open squares) contributions. The lines are quadratic fits as guide to the eye.

a factor of $\sim$1.5 compared to the highest value of the two end compounds. Thus, alloying of these chalcopyrite crystals could be useful to obtain higher values of $\chi^{(2)}$.

V. CONCLUSIONS

Calculations were performed for $Cu_{1-x}Ag_xGaS_2$ alloys based on the chalcopyrite structure with random and layered structures in the group-I sublattice. A large band-gap bowing, with bowing parameter $b=0.7$ eV, was obtained both for layered and special quasirandom structures. It was found, however, that the c/a ratio has an important contribution to the bowing. The c/a ratio varies nonlinearly with concentration itself and this apparently increases the bowing parameter from about $0.5-0.7$ eV. The pure volume deformation contribution to the bowing was found to be only 0.2 eV. Thus, the chemical mixing and relaxation contributions are the dominant contributions to the band-gap bowing. The strong band-gap bowing coefficient also leads to a nonlinear behavior of the indices of refraction, which are found to exhibit an upward bowing but with little change in birefringence. The second-order optical susceptibility $\chi^{(2)}$ is also found to have an upward bowing and reaches a maximum for a concentration near 50%.

ACKNOWLEDGMENTS

[1] K. Ramanathan, M. A. Contreras, C. L. Perkins, S. Asher, F. S. Hasoon, J. Keane, D. Young, M. Romero, W. Metzger, R. Noufi, J. Ward, and A. Duda, Prog. Photovoltaics **11**, 225 (2003).

[2] G. C. Catella and D. Burlage, Mater. Res. Bull. **23**, 28 (1998), and references therein.

[3] S. B. Zhang, S.-H. Wei, A. Zunger, and H. Katayama-Yoshida,

Phys. Rev. B **57**, 9642 (1998).

[4] I.-H. Choi, S.-H. Eom, and P. Y. Yu, J. Appl. Phys. **87**, 3815 (2000).

[5] H. Matsushita, S. Endo, and T. Irie, Jpn. J. Appl. Phys., Part 2 **32**, L1049 (1993).

[6] T. Tinoco, M. Quintero, and C. Rincon, Phys. Rev. B **44**, 1613

(1991).

[7] S. Park, S. K. Lee, J. Y. Lee, J.-E. Kim, H. Y. Park, H.-L. Park, H.-J. Lim, and W. T. Kim, J. Phys.: Condens. Matter **4**, 579 (1992).

[8] P. Hohenberg and W. Kohn, Phys. Rev. **136**, B864 (1964); W. Kohn and L. J. Sham, Phys. Rev. **140**, A1133 (1965).

[9] M. Methfessel, M. van Schilfgaarde, and R. A. Casali, in *Electronic Structure and Physical Properties of Solids: The Uses of the LMTO Method*, Springer Lecture Notes, Workshop Mont Saint Odille, France, 1998, edited by Hugues Dreyssé (Springer, Berlin, 2000), pp. 114–147.

[10] E. Bott, M. Methfessel, W. Krabs, and P. C. Schmidt, J. Math. Phys. **39**, 3393 (1998).

[11] J. Harris, Phys. Rev. B **31**, 1770 (1985).

[12] W. M. C. Foulkes and R. Haydock, Phys. Rev. B **39**, 12520 (1989).

[13] D. Singh, Phys. Rev. B **43**, 6388 (1991).

[14] H. J. Monkhorst and J. D. Pack Phys. Rev. B **13**, 5188 (1976).

[15] J. E. Sipe and E. Ghahramani, Phys. Rev. B **48**, 11705 (1993).

[16] C. Aversa and J. E. Sipe, Phys. Rev. B **52**, 14636 (1995).

[17] S. N. Rashkeev, W. R. L. Lambrecht, and B. Segall, Phys. Rev. B **57**, 3905 (1998).

[18] S. N. Rashkeev and W. R. L. Lambrecht, Appl. Phys. Lett. **77**, 190 (2000).

[19] S. N. Rashkeev and W. R. L. Lambrecht, Phys. Rev. B **63**, 165212 (2001).

[20] Z. H. Levine and D. C. Allan, Phys. Rev. B **43**, 4187 (1991).

[21] P. E. Blöchl, O. Jepsen, and O. K. Andersen, Phys. Rev. B **49**, 16223 (1994).

[22] A. Zunger, S.-H. Wei, L. G. Ferreira, and J. E. Bernard, Phys. Rev. Lett. **65**, 353 (1990).

[23] J. M. Cowley, J. Appl. Phys. **21**, 24 (1950).

[24] K. A. Mäder and A. Zunger, Phys. Rev. B **51**, 10462 (1995).

[25] A. V. Ruban (private communication).

[26] A. V. Ruban, S. I. Simak, S. Shallcross, and H. L. Skriver, Phys. Rev. B **67**, 214302 (2003).

[27] I. A. Abrikosov, S. I. Simak, B. Johansson, A. V. Ruban, and H. L. Skriver, Phys. Rev. B **56**, 9319 (1997).

[28] B. Alling, A. V. Ruban, A. Karimi, O. E. Peil, S. I. Simak, L. Hultman, and I. A. Abrikosov, Phys. Rev. B **75**, 045123 (2007).

[29] H. Neumann, Phys. Status Solidi A **96**, K121 (1986).

[30] L. Vegard, Z. Phys. **5**, 17 (1921).

[31] J. E. Jaffe and A. Zunger, Phys. Rev. B **29**, 1882 (1984).

[32] A. Zunger and J. E. Jaffe, Phys. Rev. Lett. **51**, 662 (1983).

[33] S. C. Abrahams and J. L. Bernstein, J. Chem. Phys. **61**, 1140 (1974).

[34] S. K. Kurtz, J. Jerphagnon, and M. M. Choy, in *Elastic, Piezoelectric, Pyroelectric, Piezooptic, Electrooptic Constants, and Nonlinear Dielectric Susceptibilities of Crystals*, Landolt-Börnstein, New Series, Group III, Vol. 11, edited by K.-H. Hellwege and A. M. Hellwege (Springer, Berlin, 1979), p. 671.